Journal of Ocean and Wind Energy (ISSN 2310-3604)

Vol. 2, No. 1, February 2015, pp. 45–53

http://www.isope.org/publications

Numerical Study of Interactions Between Phase II of OC4 Wind Turbine and Its Semi-Submersible Floating Support System

Wenchao Zhao and Decheng Wan
State Key Laboratory of Ocean Engineering, School of Naval Architecture, Ocean and Civil Engineering
Shanghai Jiao Tong University, Shanghai, China

The motion response of the floating support system is critical in designing and confirming the safety and efficiency of an offshore wind turbine. This paper aims to study the interaction between the wind turbine and its semi-submersible floating system for Phase II of the Offshore Code Comparison Collaboration Continuation (OC4) project. First, the validation of wave generation and damping is performed to guarantee the accuracy of waves. Then, the grid convergence is studied to eliminate the influence of different grids. Last, the motion of the semi-submersible floating system in specific waves is compared with a parked wind turbine and with an equivalent operated wind turbine. The equivalent forces and moments of the NREL 5-MW in different wind speeds have been exerted on the rotational center of the semi-submersible floating system. The results show the influences of the wind turbine on the supporting system in waves.

INTRODUCTION

Rapid economic development results in a growing demand for energy. However, traditional energy, such as fossil fuels, has been overexploited, with many environmental and climate problems arising. Nowadays, more and more attention is being paid to new energies to settle the increasingly urgent energy crisis. The clean, renewable and recyclable features of wind energy have been focused on. It is widely recognized that wind energy is the most promising energy among all of the new renewable energies. Many European countries, such as Denmark and the Netherlands, have devoted a large sum of resources to study the utilization of wind energy. Compared with onshore wind energy, offshore wind energy has more advantages, such as high wind speed, stable wind, weak wind shear, and little visual and noise pollution (Zhao and Gong, 2013). With the first offshore wind farm constructed in Sweden in 1990, offshore wind energy began its rapid development. At the end of 2012, the installed capacity of offshore wind power has reached 5 million kilowatts in Europe, and it is planned to reach 40 million kilowatts in 2020 and 150 million kilowatts in 2030 (Zhao and Gong, 2013).

The reliability of the supporting platform is a critical factor in the safety design of the offshore wind turbine. At sea, the wind turbine may encounter a variety of wind and wave conditions. The dynamic response of the support system in different circumstances deserves extensive study to maintain security and reliability. Research on the floating foundations has been conducted since the 1990s (Tang et al., 2011). Zhang et al. (2012) analyzed some key dynamic problems and risk factors of the floating structure for working load caused by turbine running and sea environment loads of the floating structure. Roddier et al. (2010) investigated the WindFloat, a floating foundation for offshore wind turbines. Goupee et al. (2012) tested three different floating wind turbine configurations in a wave basin under combined wind/wave loading. There are three common floating foundations of the offshore wind turbine: the tension leg platform, the spar foundation, and the semi-submersible platform (Sclavounos, 2008). Gao et al. (2013) adopted the boundary element method and combined with multi-body dynamics, analyzing the motion response and wave force mechanism of the tension leg platform of a floating offshore wind turbine. Utsunomiya et al. (2009) carried out an experimental validation for motion of a 2-MW SPAR-type floating offshore wind turbine. Coulling et al. (2013) validated a model constructed in the National Renewable Energy Laboratory (NREL) floating wind turbine simulator FAST with 1/50th-scale model test data for a semi-submersible floating wind turbine system.

The three-column semi-submersible floating platform is used in Phase II of the Offshore Code Comparison Collaboration Continuation (OC4) project (Robertson et al., 2012), which is a verification of modeling by comparing results of simulated responses between tools. Many research works have been done on this platform. Chung (1976) computed the hydrodynamic forces and six degree-of-freedom motion about the famous three-column semi-submersible SEDCO-135 platform with a potential flow theory. Chung (1994) provided experimental data of large-model added mass and damping that commercial programs WADAM and WAMIT cannot match or validate for the three-column semi-submersible platform. Luan et al. (2013) used a novel modeling method based on the code Simo/Riflex to simulate force and moment response in the brace system of a semi-submersible wind turbine. Koo et al. (2014) carried out a model test on three different floating platforms: a spar, a semisubmersible, and a tension-leg platform (TLP). The purpose was to generate data on coupled motions and loads between the three floating platforms and the same wind turbine for the operational, design, and survival sea states. Li et al. (2015) presented an aero-hydro Matlab code for the dynamic analysis of an offshore floating wind turbine and validated with a model test carried out in the Deepwater Offshore Basin at Shanghai Jiao Tong University. However, most research models are 1/50th-scale models, and the research method is based on potential theory. CFD methods in viscous flow fields are not common, but are studied in this project.

The wind turbine for OC4 Phase II will be the National Renewable Energy Laboratory (NREL) offshore 5-MW baseline wind turbine (Jonkman et al., 2009), which has abundant experimental data and simulation results. The aim of this paper is to investigate

Received November 8, 2014; updated and further revised manuscript received by the editors January 4, 2015. The original version (prior to the final updated and revised manuscript) was presented at the Twenty-fourth International Ocean and Polar Engineering Conference (ISOPE-2014), Busan, Korea, June 15–20, 2014.
KEY WORDS: Offshore wind turbine, semi-submersible floating system, OC4, numerical simulation, naoe-FOAM-SJTU solver.

the NREL 5-MW wind turbine impacts on its semi-submersible floating support system for Phase II of OC4 in specified wave conditions based on our own code naoe-FOAM-SJTU solver. The equivalent method is used to investigate the impacts of the NREL 5-MW wind turbine. The equivalent forces and moments are exerted on the rotational center of the floating support system, assuming that the wind turbine is working. The forces and motions of the semi-submersible floating system have been compared with a parked wind turbine and with an equivalent operated wind turbine. As Phase II of the OC4 project has no experimental data nowadays, the results of this paper are only self-validated. Despite this, our group has done a lot of work to clarify the reliability in dealing with aerodynamics of the wind turbine (Wang et al., 2012) and the dynamic responses of the platform in different waves (Liu and Wan, 2013). In this paper, naoe-FOAM-SJTU solver will be described first. Next, the geometry model, governing equations, and discretization schemes are introduced to configure the cases in different wind speeds. In addition, the wave generation and damping validation are used to show the accuracy of the numerical wave tank. Grid convergence is also used to clarify the independence of the grid. Then, the results are compared to show the impacts of the NREL 5-MW wind turbine. Finally, a conclusion is drawn.

NUMERICAL SIMULATION

naoe-FOAM-SJTU Solver

The solver adopted in this paper is our own code naoe-FOAM-SJTU (Shen, Cao, and Wan, 2012) (hereafter referred to as Solver 1), which is based on open source code OpenFOAM platform. Solver 1 was developed to deal with the hydrodynamic problems of naval architecture and ocean engineering in which the RANS equations are discretized by finite volume method, the surface interface is captured by VOF method, and motions of ship and ocean structures in waves are handled by dynamic deformation mesh approach (Shen, Ye, and Wan, 2012). This solver has several modules, such as a wave generation and damping module, six degree-of-freedom (6DoF) module, and mooring line module, to solve different problems. A numerical tank system is formed by the wave generation and damping module. Different methods such as piston, flap, and boundary inlet are used to generate first- and high-order nonlinear waves, transient extreme waves, and freak waves. Cha and Wan (2011) first achieved the piston-type and flap-type numerical method to obtain the linear wave and finite amplitude waves based on interDyMFoam in OpenFOAM. In order to absorb the wave at the end of the wave tank, a damping zone is set at the appropriate location. The 6DoF module, developed by Shen and Wan (2013), is used to predict the dynamic motions of ship and ocean structures in different waves. The mooring lines module is developed to handle the motion problems of floating structures in deep sea. Liu and Wan (2013) studied a series of numerical simulations of the interaction of a triple-hulled observation platform with different incident waves. Cao et al. (2013) analyzed the wave loading on a floating platform coupled with a mooring system.

Solver 1 has proved to be competent in solving the floating platform movement in waves, which provides solid support for this paper. A test case conducted by Solver 1 is presented here. The model is a deepwater semi-submersible drilling platform, as shown in Fig. 1. The parameters of the model are set in accordance with the experiment by Shi et al. (2011), which performed the white noise test, regular wave test, and numerical simulation by SESAM in multiple sets of waves. The motion response of the semi-submersible platform is simulated by Solver 1 under the effect of three different periods of incident waves. The motion response amplitude operator (RAO) of surge, heave, and pitch are

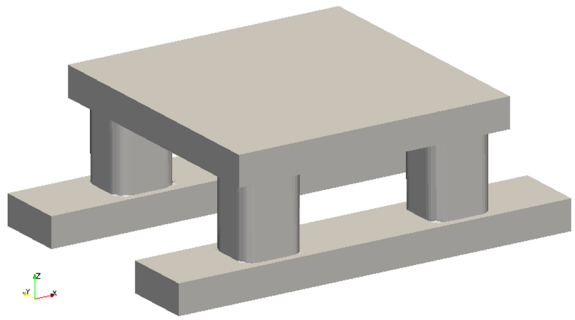

Fig. 1 Deepwater semi-submersible drilling platform model

compared with Shi et al.'s experiment and numerical results, which are shown in Figs. 2, 3, and 4. In these figures, it is clearly shown that the motion response of the semi-submersible platform in waves simulated by Solver 1 is reliable and close to the experimental results. Based on the test, in the following numerical computations, the motion response of the three-column semi-submersible platform of OC4 is numerically investigated by using the same solver.

Geometry Model

The geometry model for Phase II of the OC4 project is a semi-submersible floating offshore wind system, as shown in Fig. 5. From a report by the National Renewable Energy Laboratory (Robertson

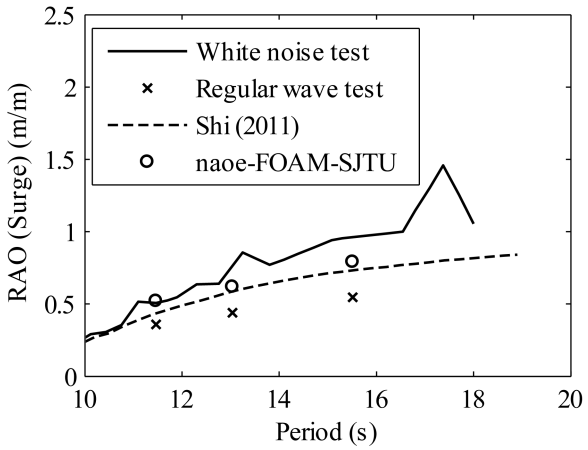

Fig. 2 Comparison of RAO (surge)

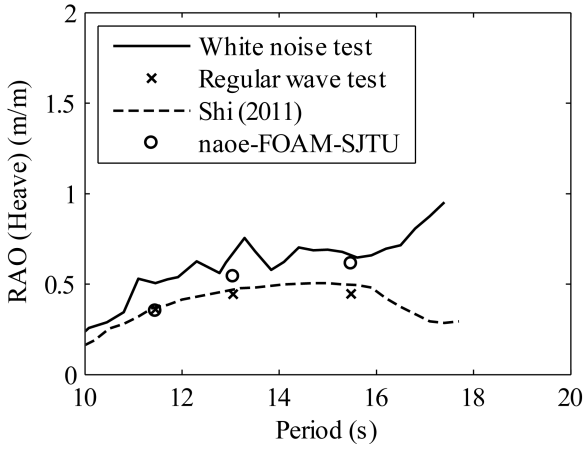

Fig. 3 Comparison of RAO (heave)

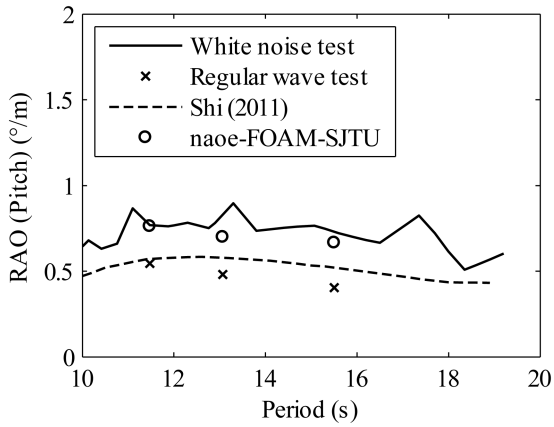

Fig. 4 Comparison of RAO (pitch)

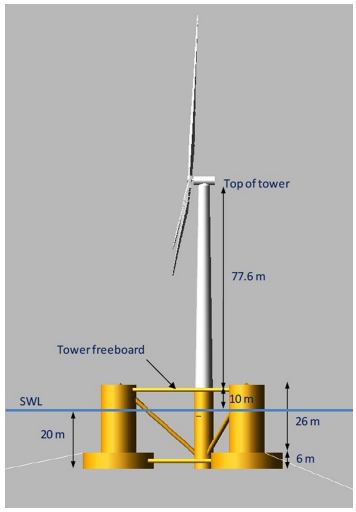

Fig. 5 DeepCwind floating wind system design

et al., 2012), the OC4 project compares dynamic computer codes and models used to design offshore wind turbines and support structures. Nowadays, many agencies and institutions are dedicated to studying this project as a floating standard model.

This paper is based on this model to explore the wind turbine impacts on the semi-submersible floating support system. As we know, the coupled solution of aerodynamic and hydrodynamic problems is very complicated. To simplify this problem, the equivalent method has been applied, which will be described in detail later. The semi-submersible design examined in this phase is based on the as-built configuration used in the DeepCwind tests,

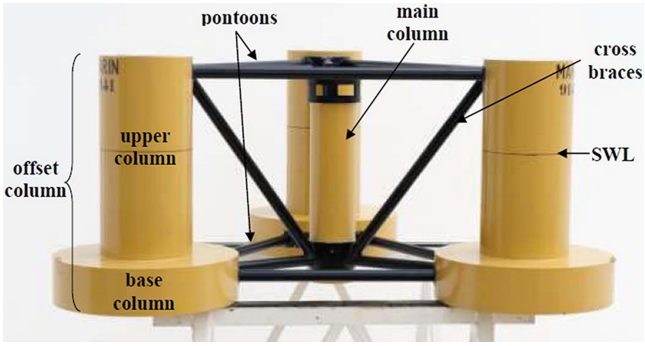

Fig. 6 As-built picture of semi-submersible floating system

Depth of platform base below SWL (total draft)	20 m
Elevation of main column (tower base) above SWL	10 m
Elevation of offset columns above SWL	12 m
Spacing between offset columns	50 m
Length of upper columns	26 m
Length of base columns	6 m
Depth to top of base columns below SWL	14 m
Diameter of main column	6.5 m
Diameter of offset (upper) columns	12 m
Diameter of base columns	24 m
Diameter of pontoons and cross braces	1.6 m

Table 1 Floating platform geometry

as shown in Fig. 6. However, the wind turbine specification for OC4 Phase II will be the National Renewable Energy Laboratory (NREL) offshore 5-MW baseline wind turbine (Jonkman et al., 2009), which is a representative multi-MW turbine. This turbine will be used in all phases of OC4.

As shown in Fig. 5, the tower is cantilevered at an elevation of 10 m above the still water lever (SWL) to the top of the main column. The draft of the platform is 20 m. The DeepCwind semi-submersible consists of a main column attached to the tower plus three offset columns that are connected to the main column through a series of smaller-diameter pontoons and cross members. The parameters of this floating platform, including the diameters of each of the members, are given in Table 1.

Forces and Moments of Equivalent Wind Turbine

This paper uses the equivalent method to study wind turbine impacts on its semi-submersible floating support system. Referring to the NREL 5-MW wind turbine, the average of forces and moments of the wind turbine at different wind speeds are exerted on the rotational center of the semi-submersible floating system. Figure 7 shows the results from the NREL of the wind turbine at different wind speeds (Jonkman et al., 2009). A steady-state response of the land-based 5-MW wind turbine is done by running a series of FAST (an aeroelastic computer-aided engineering (CAE) tool for horizontal axis wind turbines) (Jonkman and Buhl Jr, 2005) with AeroDyn (aerodynamics analysis routines for horizontal-axis wind turbine dynamics analyses) (Moriarty and Hansen, 2005) simulations at a number of given, steady, and uniform wind speeds. The steady-state results are suggested by NREL to mitigate the start-up transient behavior, which is an artifact of computational analysis.

In Fig. 7, RotThrust represents the rotor thrust, and RotTorq represents the mechanical torque in the low-speed shaft. The rotor

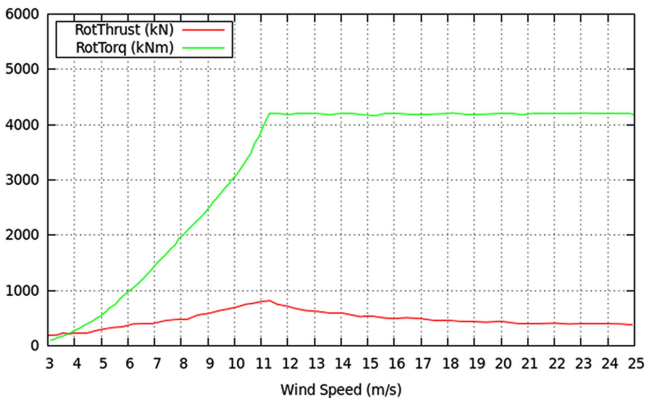

Fig. 7 Forces and moments of NREL 5-MW wind turbine

thrust and torque of wind speeds 5 m/s, 7 m/s, and 11.4 m/s have been picked up. However, the data are measured at the rotational center of the blades, which is located 87.6 m above the SWL. Thus, the theorem of translation of force has been applied to compute the forces and moments about the rotational center of the semi-submersible floating supporting system. There will be an additional torque generated in the translation of a force.

The formulas of this theorem are:

$$\vec{F}' = \vec{F} \tag{1}$$

$$\vec{M}' = \vec{M} + r \times \vec{F} \tag{2}$$

where r is the distance between the center of the blades and the rotational center of the semi-submersible floating support system, $\vec{F}$ and $\vec{M}$ are the forces and moments obtained from the experimental data, and $\vec{F}'$ and $\vec{M}'$ are the forces and moments exerted on the support system.

Governing Equations

In order to solve the unsteady, incompressible, and viscous fluid, the three-dimensional incompressible Reynolds-Averaged Navier-Stokes (RANS) equations are chosen as the governing equations, which can be written in vector form as:

$$\nabla \cdot U = 0 \tag{3}$$

$$\frac{\partial \rho U}{\partial t} + \nabla \cdot (\rho U U) = -\nabla p - g \cdot x \nabla \rho + \nabla \cdot (\mu_{\text{eff}} \nabla U) + (\nabla U) \cdot \nabla \mu_{\text{eff}} + f_\sigma \tag{4}$$

where U is the velocity field; ρ is the density of the fluid; g is the acceleration due to gravity; p is the pressure; $\mu_{\text{eff}} = \rho(\nu + \nu_t)$ is the efficient dynamic viscosity, in which ν is the kinematic viscosity and ν_t is the turbulence kinetic viscosity, which is given by the SST k-ω turbulence model (Menter, 1994); f_σ is the surface tension term in two-phase model.

The solution of the governing equations is obtained with a new algorithm called PIMPLE (merged PISO-SIMPLE), which is a combination of pressure-implicit split-operator (PISO) proposed by Issa (1986) and semi-implicit method for pressure-linked equations (SIMPLE) proposed by Patankar and Spalding (1972), to decouple the pressure-velocity coupling equation. This algorithm regards the flow as a steady-state flow at each time step, then uses the standard PISO algorithm to complete the progressive of the time step, which accelerates the convergence time of the whole process of solving.

Discretization Schemes

The governing equations are discretized based on the Finite Volume Method (FVM) (Versteeg and Malalasekera, 2007). The unsteady term applies the Euler scheme. The Gauss limitedLinearV 1 scheme is employed to discretize the convective term, while the Gauss linear corrected is used to discretize the diffusive term. The VOF method (Hirt and Nichols, 1981) is adopted in Solver 1 to track the free surface, which is discretized by the Gauss vanLeer scheme. The gradient term uses the Gauss linear scheme, and the interpolation term applies the linear scheme.

NUMERICAL RESULTS

Model Configurations

The purpose of this paper is to study the wind turbine impacts on its semi-submersible floating system in waves. The water depth d is determined as 200 m. According to the practical periodic sea states defined in Table 2 (from 1 = mild to 8 = extreme sea state), the sea state 5 has been chosen as the wave condition used in this paper.

Sea state	T (s)	H (m)
1	2.0	0.09
2	4.8	0.67
3	6.5	1.40
4	8.1	2.44
5	9.7	3.66
6	11.3	5.49
7	13.6	9.14
8	17.0	15.24

Table 2 Periodic sea state definitions

As seen in Table 2, the specific wave height H is 3.66 m and the period T is 9.7 s, which is a strong wave condition. According to the wave theory, the wave length L, the wave number k, and the frequency ω can be acquired by formulas below:

$$L = \frac{gT^2}{2\pi} = 146.9 \text{ m} \tag{5}$$

$$k = \frac{2\pi}{L} = 0.04277 \text{ m}^{-1} \tag{6}$$

$$\omega = \frac{2\pi}{T} = 0.64775 \text{ s}^{-1} \tag{7}$$

As the wave length L is 146.9 m and the water depth d is 200 m, the x range is set from −148 m to −280 m. In order to absorb the wave adequately at the end of the wave tank, the damping zone is set from 140 m to 280 m, close to one wave length. The width of the wave tank is 240 m and the height is set from −200 m to −50 m, as shown in Fig. 8.

This paper validates the wave generation and wave damping first to eliminate the interference of wave inaccuracy. Then the grid convergence verification is used to guarantee the independence of density of grid. Last, three sets of results (wind speeds of 5 m/s, 7 m/s, and 11.4 m/s, respectively) are compared to analyze the degree of influence on the semi-submersible floating support system. In this paper, case 1 is the floating system without the equivalent forces and moments of the wind turbine, and case 2 is the floating system including the equivalent forces and moments of the wind turbine. The model is shown in Fig. 9.

Validation of Wave Generation and Damping

The wave generation and damping are verified by the 2-D numerical wave tank, whose results can expand to the 3-D numerical

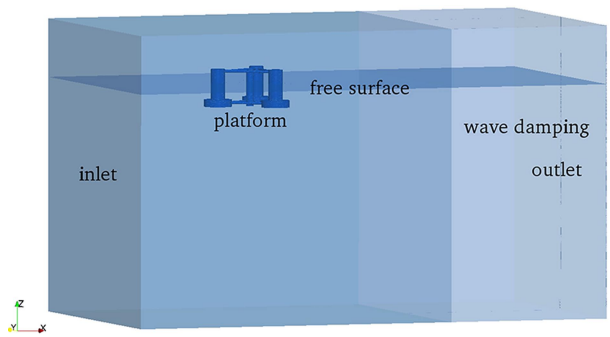

Fig. 8 Computational domain and free surface

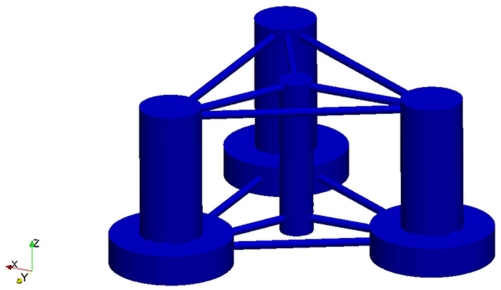

Fig. 9 Model of the semi-submersible platform

wave tank. In order to test the height of the wave generation in the different positions of the tank, four wave gauges ($x = -140$ m, 0 m, 140 m, 249 m) are set to obtain the data. The results are compared with the theoretical solution. From wave theory, the theoretical height of the wave surface of Stokes second-order can be computed by the formula below:

$$\eta = \frac{H}{2}\cos(kx - \omega t) + \frac{H}{8}\left(\frac{\pi H}{L}\right)\cdot\frac{\cosh kd}{\sinh^3 kd}(\cosh 2kd + 2)\cos(2(kx - \omega t)) \tag{8}$$

where H is the wave height, L is the wave length, d is the water depth, k is the wave number, and ω is the wave frequency. The above parameters are already known in the model configurations. By the comparison of the numerical and theoretical values, the accuracy of the wave generation and damping can be guaranteed.

Figure 10 shows the comparison results of wave elevation at four wave gauges. The first three graphs display the results of wave generation from 0 s to 150 s at the different positions. In general, the numerical simulation results and theoretical solution have high agreements except for some subtle differences in the crest and trough of the wave. The wave crests of the theoretical solution are a little higher than the numerical values due to the failure of wave theory to consider the viscosity of the fluid and the surface tension effects. On the other hand, there are nonlinearity and high-order components in the simulation process that may influence these results. The last graph is the demonstration of the wave damping area. The results illustrate that the wave height has been reduced significantly, where it is less than 10 percent of the original wave height. This shows the efficiency of the sponge layer zone. In conclusion, the wave generation and damping in this paper are accurate and reliable.

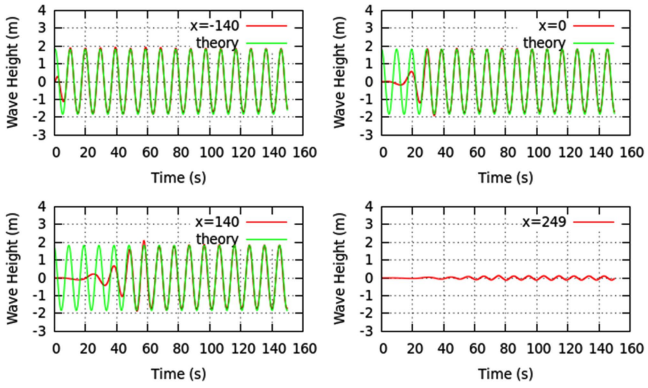

Fig. 10 Comparison of numerical and wave theory results

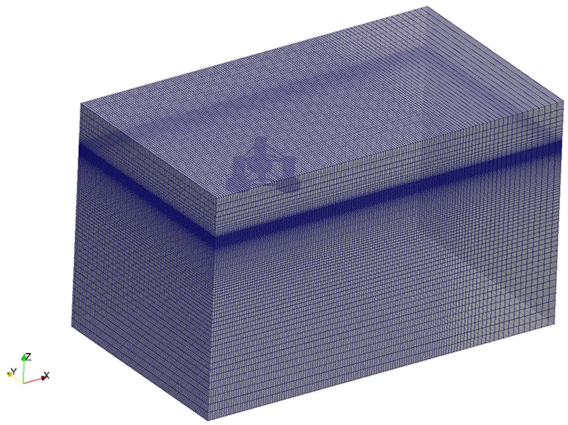

Fig. 11 Global mesh of the computational domain

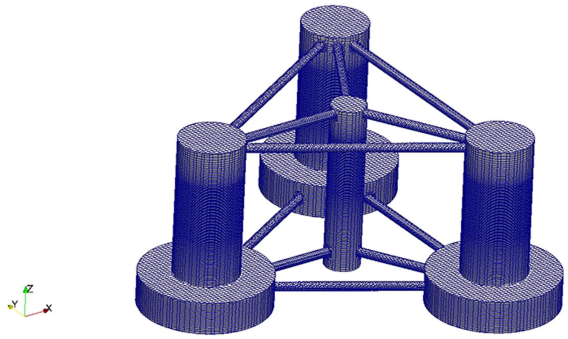

Fig. 12 Local mesh of the supporting platform

Grid Convergence Verification

Due to the limited computing resources and costs, reasonable grid numbers must be applied in the numerical simulation of this paper. The validation of the grid convergence has been done to ensure the effectiveness of the results with proper grid numbers. The mesh is generated with ANSYS ICEM-CFD software and OpenFOAM's built-in snappyHexMesh utility. The background mesh is generated by the ANSYS ICEM-CFD software. Then the mesh around the semi-submersible floating supporting system is achieved by the snappyHexMesh utility. This utility generates three-dimensional meshes containing hexahedra and split-hexahedra automatically from the STL surface. The global mesh and local mesh of the semi-submersible floating system are shown in Fig. 11 and Fig. 12, respectively.

To verify the grid convergence, three different groups of grid numbers have been compared. The grid numbers are shown in Table 3, and the comparison results are presented in Fig. 13 and Fig. 14. Mesh 1 has the most sparse grid and mesh 3 has the finest grid. By the computation of these three sets of grid numbers, numerical results are observed and analyzed. Figure 13 shows that the wave forces and moments are almost the same. In the comparison of the heave and pitch motions of the semi-submersible floating system, the results are relatively consistent, except for

Mesh type	Background grid numbers	Total grid numbers
1	885552	976590
2	1221760	1337379
3	1501552	1625359

Table 3 Three mesh types

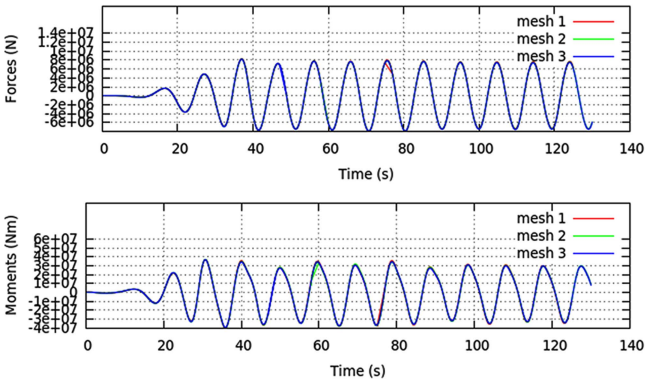

Fig. 13 Comparison of forces and moments of three mesh types

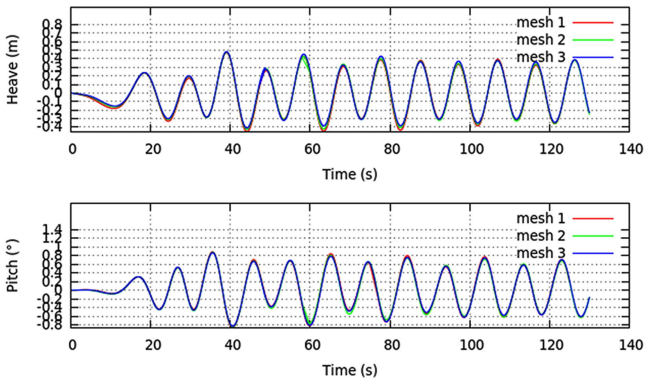

Fig. 14 Comparison of motions of three mesh types

small differences. The comparison results indicate that these three grids tend to convergence. The influence of grid numbers can be eliminated and the simulation results are reliable. Thus, mesh 2 is chosen as the final mesh to complete all the simulations below.

Forces and Moments on the Semi-Submersible Floating System

As described previously, the simulation results of case 1 and case 2 are compared when the wind speeds are 5 m/s, 7 m/s, and 11.4 m/s, respectively. First, the wave forces and moments on the semi-submersible support system at the three wind speeds are compared. The time history of the wave forces is shown in Figs. 15, 16, and 17. According to the comparison results, the wind turbine impacts on the forces and moments of the semi-submersible support system are not significant. The forces and moments of the platform change little.

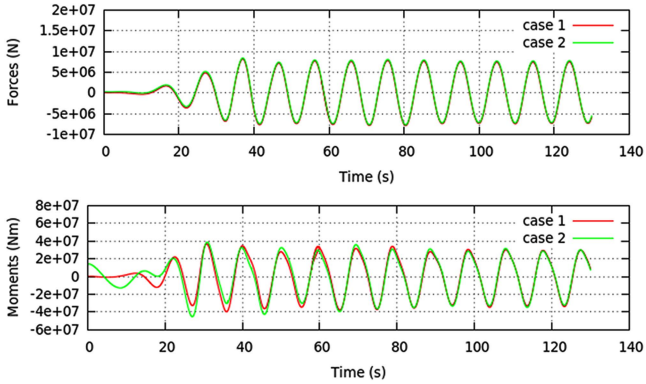

Fig. 15 Forces and moments of the platform for 5 m/s wind speed

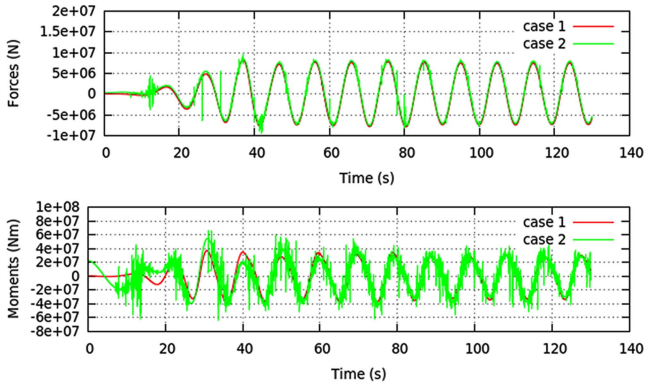

Fig. 16 Forces and moments of the platform for 7 m/s wind speed

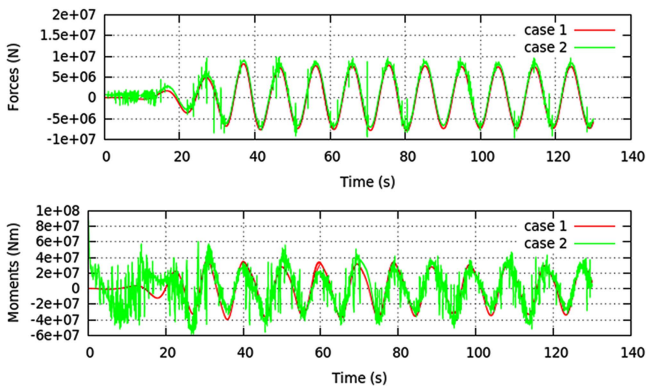

Fig. 17 Forces and moments of the platform for 11.4 m/s wind speed

Due to the initial forces and moments exerted by the equivalent wind turbine, there is an explicit difference in the beginning of the computation. Then the difference tends to be consistent. In Fig. 16 and Fig. 17, the obvious numerical oscillation is observed, which may be caused by the large movement of the platform and numerical dissipation generated by the variable time steps. Further study is needed to explore the reason leading to the numerical oscillation. Figures 15, 16, and 17 show that the wind turbine impacts on the forces and moments of the semi-submersible floating support system have little effect under the conditions of this paper.

Motions of the Supporting Platform

The semi-submersible floating support system produces heave and pitch motions. The motions in these two directions have been

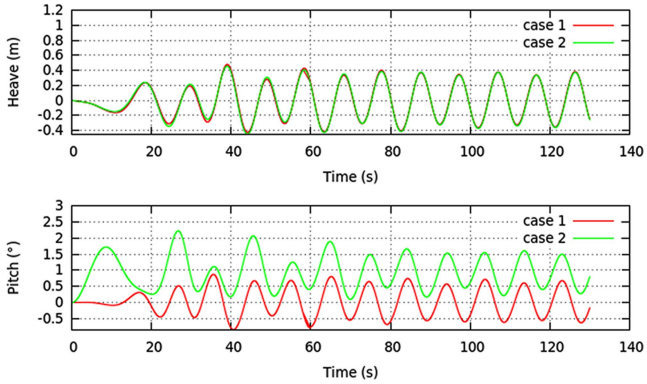

Fig. 18 Heave and pitch of the platform for 5 m/s wind speed

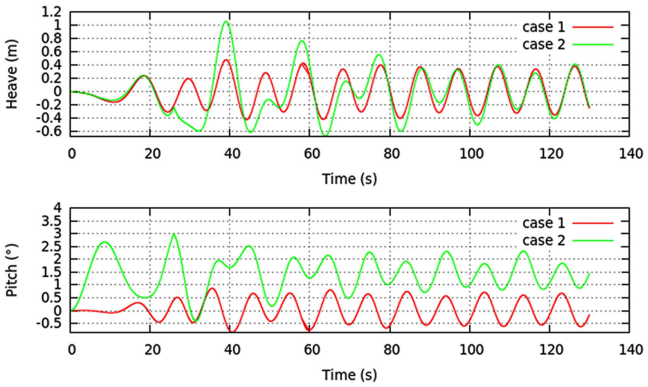

Fig. 19 Heave and pitch of the platform for 7 m/s wind speed

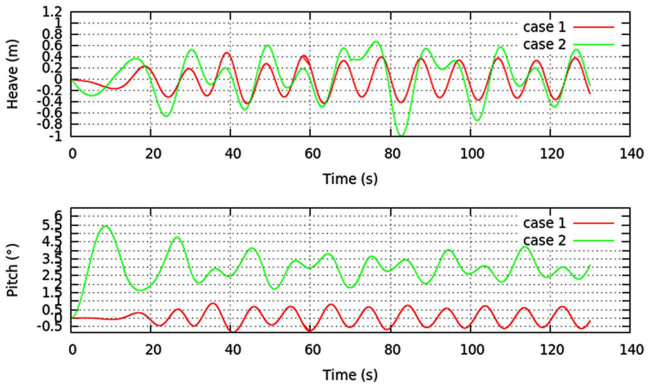

Fig. 20 Heave and pitch of the platform for 11.4 m/s wind speed

exported, and comparison is performed to clarify the degree of influence attributable to the wind turbine, as shown in Figs. 18, 19, and 20. It can be seen that the wind turbine has great impact on the movements of the semi-submersible floating support system, especially the pitch motion. When the wind speed is 5 m/s, the heave motion is almost the same with case 1. As the wind speed increases, the heave motion becomes larger with small amplitude. At a certain moment, the heave motion reaches a maximum value. However, the pitching motion changes dramatically with a higher wind speed. The pitching motion is less than 1° in case 1, while the pitch amplitude reaches nearly 6° in case 2 when the wind speed of the wind turbine is 11.4 m/s. That means that the wind turbine has a remarkable impact on the pitching motion of the semi-submersible floating support system. The supporting platform is in danger of overturning in extreme sea conditions, and the mooring line should be used under these conditions.

Velocity and Pressure of the Free Surface

In order to get detailed information about the flow field, the velocity and pressure of the free surface at four different moments during a wave period are presented in Figs. 21–24. The existence of the equivalent wind turbine has affected the velocity and pressure of the supporting structure around the free surface.

To further study the wind turbine impacts on its semi-submersible floating support system, the detailed flow field has been observed. Thus, the velocity and pressure of the free surface of case 1 and case 2 have been compared. Case 2 chooses the condition with wind speed of 11.4 m/s, where it is easier to see the impact of the equivalent wind turbine on the supporting platform. As seen in Fig. 21 and Fig. 22, the water flow behind the semi-submersible support system is different. The latter has a faster flow rate due

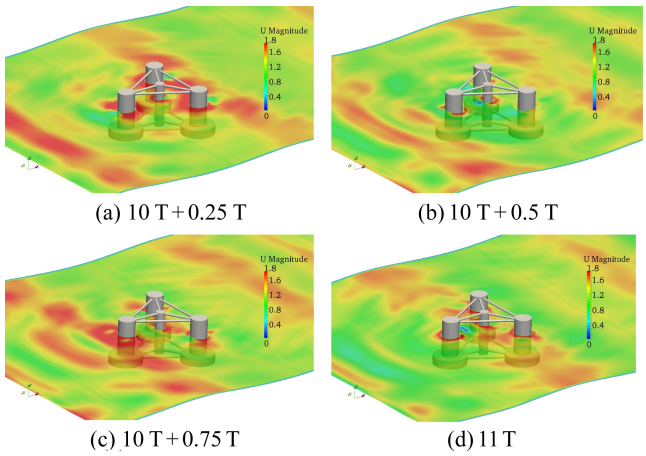

Fig. 21 Velocity of the free surface of case 1

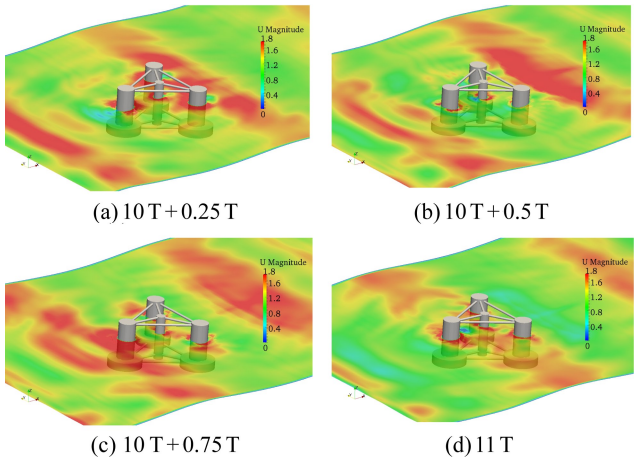

Fig. 22 Velocity of the free surface of case 2

to the substantial movement of the supporting platform. It is demonstrated that the platform with the wind turbine will suffer more severe sea conditions than the platform itself. The impact cannot be ignored.

Figures 23 and 24 show the pressure chart of the free surface. On the whole, the differences in the pressure distribution about the free surface are not obvious. However, the clear pressure variation of the free surface during a period deepens the understanding of

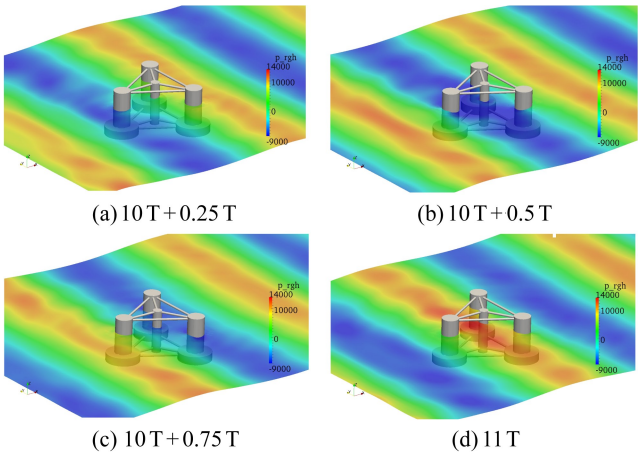

Fig. 23 Pressure of the free surface of case 1

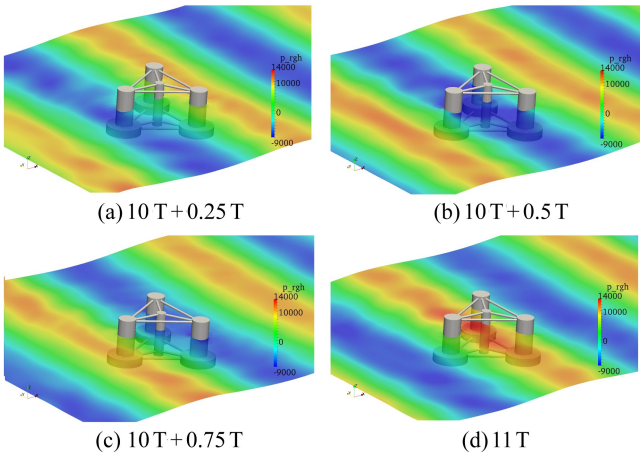

(a) 10 T + 0.25 T (b) 10 T + 0.5 T

(c) 10 T + 0.75 T (d) 11 T

Fig. 24 Pressure of the free surface of case 2

the pressure field. More work should be done to discuss the other conditions where wind speeds are higher.

CONCLUSIONS

In this paper, the wind turbine impacts on its semi-submersible floating support system in a specific wave have been studied with our naoe-FOAM-SJTU solver. To solve the coupling of aerodynamic and hydrodynamic problems of the floating platform and wind turbine, an equivalent method has been adopted. The equivalent forces and moments of the NREL 5-MW wind turbine were exerted on the semi-submersible floating system. The results of three wind speeds have been compared. To ensure the reliability of the simulation results, wave generation and damping have been verified, and grid convergence study has been performed.

In order to analyze the wind turbine impacts on its semi-submersible floating support system, the numerical simulation results of case 1 and case 2 have been compared. As shown above, the wind turbine leads to substantial movement of the semi-submersible platform, especially the pitch motion. It can remind the designers to strengthen the safety design of the platform of the floating wind turbine at sea. In addition, the flow information intuitively displays the velocity and pressure changes of the free surface and the impacts of the wind turbine. The wind turbine mainly affects the velocity field of the free surface behind the supporting platform.

The conclusion can be made that the wind turbine has apparent impacts on its semi-submersible floating support system in waves, especially the pitch motion at high wind speed. This paper is a preliminary exploration of the wind turbine impacts on its floating support system. Subject to constraints, the mooring lines were not added to the semi-submersible support system. In the future, the dynamic response of the floating platform of the wind turbine with mooring lines is a promising research direction. Much further work should be performed to investigate this problem.

ACKNOWLEDGEMENTS

The authors are most grateful for the support of this work from the National Natural Science Foundation of China (Grant Nos. 51379125, 51411130131, and 11432009), the National Key Basic Research Development Plan (973 Plan) Project of China (Grant No. 2013CB036103), the High Technology of Marine Research Project of The Ministry of Industry and Information Technology of China, the Program for Professor of Special Appointment (Eastern Scholar) at Shanghai Institutions of Higher Learning (Grant No. 2013022), ABS (China), and the Center for HPC at Shanghai Jiao Tong University.

REFERENCES

Cao, HJ, Wang, XY, Liu, YC, and Wan, DC (2013). "Numerical Prediction of Wave Loading on a Floating Platform Coupled with a Mooring System," *Proc 23rd Int Offshore Polar Eng Conf*, Anchorage, AK, USA, ISOPE, 3, 582–589.

Cha, JJ, and Wan, DC (2011). "Numerical Wave Generation and Absorption Based on OpenFOAM," *China Ocean Eng*, 29(3), 1–12.

Chung, JS (1976). "Motion of a floating structure in water of uniform depth," *J Hydronaut*, AIAA, 10(3), 65–73.

Chung, JS (1994). "Added Mass and Damping on an Oscillating Surface-Piercing Circular Column with a Circular Footing," *Int J Offshore Polar Eng*, ISOPE, 4(1), 11–17.

Coulling, AJ, Goupee, AJ, Robertson, AN, Jonkman, JM, and Dagher, HJ (2013). "Validation of a FAST Semi-Submersible Floating Wind Turbine Numerical Model with DeepCwind Test Data," *J Renewable Sustainable Energy*, 5(2), 023116.

Gao, YW, Li, C, and Cheng, X (2013). "Performance Research on Tension Leg Platform of Floating Offshore Wind Turbine," *Adv Mater Res*, 724–725, 645–648.

Goupee, AJ, Koo, B, Lambrakos, K, and Kimball, R (2012). "Model Tests for Three Floating Wind Turbine Concepts," Presented at *Offshore Technology Conference*, Houston, TX, USA, http://dx.doi.org/10.4043/23470-MS.

Hirt, CW, and Nichols, BD (1981). "Volume of Fluid (VOF) Method for the Dynamics of Free Boundaries," *J Comput Phys*, 39(1), 201–225.

Issa, RI (1986). "Solution of the Implicitly Discretized Fluid Flow Equations by Operator-Splitting," *J Comput Phys*, 62(1), 40–65.

Jonkman, JM, and Buhl Jr, ML (2005). *FAST User's Guide*, Technical Report NREL/EL-500-38230, National Renewable Energy Laboratory, Golden, CO, USA.

Jonkman, JM, Butterfield, S, Musial, W, and Scott, G (2009). *Definition of a 5-MW Reference Wind Turbine for Offshore System Development*, Technical Report NREL/TP-500-38060, National Renewable Energy Laboratory, Golden, CO, USA.

Koo, BJ, Goupee, AJ, Kimball, RW, and Lambrakos, KF (2014). "Model Tests for a Floating Wind Turbine on Three Different Floaters," *J Offshore Mech Arct Eng*, 136(2), 021904.

Li, L, Hu, ZQ, Wang, J, and Ma, Y (2015). "Development and Validation of an Aero-hydro Simulation Code for Offshore Floating Wind Turbine," *J Ocean Wind Energy*, ISOPE, to be published February 2015.

Liu, YC, and Wan, DC (2013). "Numerical Simulation of Motion Response of an Offshore Observation Platform in Waves," *J Mar Sci Appl*, 12(1), 89–97.

Luan, C, Gao, Z, and Moan, T (2013). "Modelling and Analysis of a Semi-Submersible Wind Turbine with a Central Tower with Emphasis on the Brace System," *Proc 32nd Int Conf Ocean Offshore Arct Eng*, Nantes, France, ASME, 8, V008T09A024.

Menter, FR (1994). "Two-Equation Eddy-Viscosity Turbulence Models for Engineering Applications," *AIAA J*, 32(8), 1598–1605.

Moriarty, PJ, and Hansen, AC (2005). *AeroDyn Theory Manual*, Technical Report NREL/TP-500-36881, National Renewable Energy Laboratory, Golden, CO, USA.

Patankar, SV, and Spalding, DB (1972). "A Calculation Procedure for Heat, Mass and Momentum Transfer in Three-Dimensional Parabolic Flows," *Int J Heat Mass Transfer*, 15(10), 1787–1806.

Robertson, A, et al. (2012). *Definition of the Semisubmersible Floating System for Phase II of OC4*, Technical Report NREL/TP-5000-60601, National Renewable Energy Laboratory, Golden, CO, USA.

Roddier, D, Cermelli, C, Aubault, A, and Weinstein, A (2010). "WindFloat: A Floating Foundation for Offshore Wind Turbines," *J Renewable Sustainable Energy*, 2(3), 033104.

Sclavounos, P (2008). "Floating Offshore Wind Turbines," *Mar Technol Soc J*, 42(2), 39–43.

Shen, ZR, and Wan, DC (2013). "RANS Computations of Added Resistance and Motions of Ship in Head Waves," *Int J Offshore Polar Eng*, ISOPE, 23(4), 263–271.

Shen, ZR, Cao, HJ, and Wan, DC (2012). *Manual of CFD Solver for Ship and Ocean Engineering Flows: naoe-FOAM-SJTU*, Technical Report for Solver Manual, Shanghai Jiao Tong University, Shanghai, China.

Shen, ZR, Ye, HX, and Wan, DC (2012). "Motion Response and Added Resistance of Ship in Head Waves Based on RANS Simulations," *Chin J Hydrodyn Ser A*, 27(6), 621–633.

Shi, QQ, Yang, JM, and Xiao, LF (2011). "Research on Motion and Hydrodynamic Characteristics of a Deepwater Semi-Submersible by Numerical Simulation and Model Test," *The Ocean Engineering*, 29(4), 29–36.

Tang, Y, Hu, J, and Liu, L (2011). "Study on the Dynamic Response for Floating Foundation of Offshore Wind Turbine," *Proc 30th Int Conf Ocean Offshore Arct Eng*, Rotterdam, Netherlands, ASME, 5, 929–933.

Utsunomiya, T, Sato, T, Matsukuma, H, and Yago, K (2009). "Experimental Validation for Motion of a Spar-Type Floating Offshore Wind Turbine Using 1/22.5 Scale Model," *Proc 28th Int Conf Ocean Offshore Arct Eng*, Honolulu, HI, USA, ASME, 4, 951–959.

Versteeg, HK, and Malalasekera, W (2007). *An Introduction to Computational Fluid Dynamics: The Finite Volume Method*, Pearson Education, 503 pp.

Wang, Q, Zhou, H, and Wan, DC (2012). "Numerical Simulation of Wind Turbine Blade-Tower Interaction," *J Mar Sci Appl*, 11(3), 321–327.

Zhang, RY, Chen, CH, Tang, YG, and Huang, XY (2012). "Research Development and Key Technical on Floating Foundation for Offshore Wind Turbines," *Adv Mater Res*, 446, 1014–1019.

Zhao, XL, and Gong, WM (2013). "Development of Floating Offshore Wind Turbine and the Mooring System," *Adv Mater Res*, 790, 634–637.